A Fast Noniterative Visually Lossless Compression of Dental Images Using AGU-M Coder

Olha Krylova, Liudmyla Kryvenko
Department of Therapeutic Dentistry,
Department of Pediatric Dentistry and Implantology
Kharkiv National Medical University
Kharkiv, Ukraine
krylovaol@ukr.net,
ls.kryvenko@knmu.edu.ua

Sergey Krivenko, Vladimir Lukin
Department of Information and Communication Technologies
National Aerospace University "KhAI"
Kharkiv, Ukraine
lukin@ai.kharkov.com

***Abstract*—This paper deals with lossy compression of medical images in dentistry. For this purpose, we use AGU-M coder based on discrete cosine transform. A peculiarity of the proposed approach is that visually lossless compression is carried out without iterations and, due to this, in a fast way. Invisibility of introduced distortions and/or artifacts is provided by a proper setting of a fixed scaling factor that controls compression. This allows reaching a desired quality of compressed images characterized by PSNR-HVS-M. Experiments are performed for a set of dental images produced by Morita imaging system. Image visual quality has been analyzed by a group of dentistry experts. It is shown that the proposed approach provides several benefits compared to earlier designed counterparts, in particular, a larger compression ratio.**

Keywords—image quality, lossy compression, dentistry, noise properties.

I. INTRODUCTION

Images of various origin are widely used in numerous modern applications including CAD [1], remote sensing [2], infocommunications [3], e-learning [4], non-destructive control [5]. Recently, the abbreviation CAD has also become used for computer aided diagnosis [6]. In general, imaging and image analysis have been employed in medicine for many years and in various areas [6-12]. Dentistry is a typical area where imaging and image analysis are widely exploited [12, 13]. Volume of acquired data in special clinics and diagnostic centers increases quickly because of two main reasons. First, mean image size increases due to improvement of spatial resolution of imaging systems. Fig. 1 shows examples of dental images acquired in two modes of operation of Morita system, panoramic X-ray (Veraviewepocs 3D R100 J) [14]. The size of the image in Fig. 1, a is 2625x2304 whilst the size of the image in Fig. 1, b is 2761x1504. Second, a lot of images can be acquired each day. So, it can be a problem to send several images in one mail to a given patient or expert or to store all acquired images.

Due to this, image compression is widely used in medicine in general [15-17] and in radiology imaging in particular [18-20]. Lossless compression (archiving) usually does not produce a desired effect of sufficient reduction of image(s) size. Because of this, lossy compression is used. However, in medical imaging applications lossy compression should be employed with a special care not too loose important diagnostic information.

Because of this, several approaches have been designed. One of them is to limit the compression ratio (CR) for a given type of medical images [18, 19, 21] to avoid too large distortions. Such approach does not adapt to image content or noise properties and, due to this, all possible benefits cannot be reached.

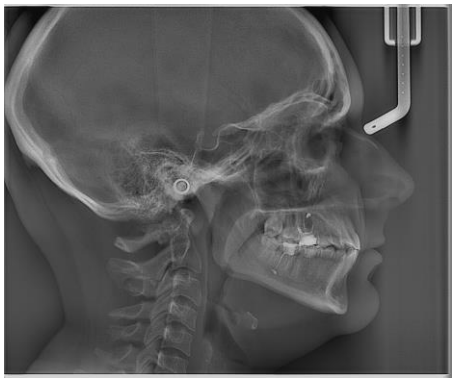

a

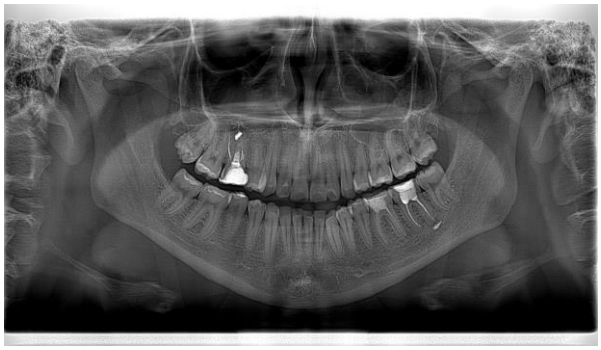

b

Fig. 1. Examples of large size dental images acquired in different modes

Another approach can be based on visual quality metrics [3, 20, 22, 23]. This approach presumes the following statements. First, visual quality metrics are able to adequately characterize image quality [3, 22]. Second, there are threshold values that correspond to invisibility of introduced distortions under condition of the largest possible CR. Third, there are reasonably fast ways to reach these threshold values with appropriate accuracy.

Currently, there are quite many visual quality metrics that correlate with mean opinion score well [3, 23]. In particular, for grayscale images, these are multiscale SSIM (MS SSIM) [24] and peak signal-to-noise ratio with taking into account human vision system and masking (PSNR-HVS-M) [25]. Distortion invisibility threshold values for these metrics have been approximately determined. For MS SSIM, distortions

are practically invisible is MS SSIM is larger than 0.985 (the maximal value of MS SSIM equals to unity and relates to perfect quality). For PSNR-HVS-M, the threshold is about 41 dB – larger values of PSNR-HVS-M practically guarantee that distortions cannot be noticed [23].

There are iterative procedures [26] that presume multiple image compression, decompression, metric determination and coder parameter changing that provide a desired metric value with very high quality. A drawback of this approach is that number of iteration can be quite large and a priori unknown. Due to this, compression might take a lot of time and be inappropriate for practice especially if a used coder is not fast enough [20]. To get around this shortcoming, a fast non-iterative procedure has been recently proposed in [20] for advanced DCT-based coder (ADCTC) [27]. This coder employs optimized partition scheme and, due to this, provides high efficiency of image compression according to peak signal-to-noise ratio (PSNR) [26]. However, it is less fast (especially at compression stage when partition scheme is optimized) compared to JPEG and JPEG2000. As the result of analysis in [20], the recommendation to set quantization step (QS) equal to 12 is given and CR in the limits from 7 to 21 for 512x512 pixel fragments is provided. The ensured PSNR-HVS-M is in the limits from 40.5 to 46.9 dB, i.e. distortions are invisible. This has been proven by experiments carried out by dentists.

Meanwhile, the results presented in [26] show that it is possible to expect better results from compression techniques oriented on providing high quality according to visual quality metrics. One of them is AGU-M [26] that uses DCT in 32x32 pixel blocks, employs efficient bit plain coding of quantized DCT coefficients and embedded deblocking after decompression. Benefits of AGU-M deal with non-equal quantization of DCT coefficients that takes into account peculiarities of HVS.

Meanwhile, advantages of AGU-M have been demonstrated in [26] for noise-free images. Real-life X-ray dental images are noisy [28] and this fact can influence performance of AGU-M. Therefore, the goal of this paper is to carefully analyze performance characteristics of AGU-M for dental images and compare them to results earlier presented in [20]. Another goal is to give practical recommendations on setting the scaling factor for AGU-M to guarantee that distortions are invisible.

II. Peculiarities of Image Lossy Compression

Lossy compression techniques are characterized by the so-called rate-distortion curves. These rate distortion curves can be expressed in various ways, as dependence of some indicator of image quality on some parameter describing compression. As an indicator of image quality, PSNR is most often used although visual quality metrics can be employed as well. As parameter describing compression, CR or bpp (bits per pixel) are most often used although parameters that control compression (PCC) like quantization step (QS) in ADCTC, scaling factor (SF) or quality factor (QF) like in JPEG can be employed as well. This is because CR is connected with these parameters. A larger CR corresponds to a larger QS, SF or QF.

A. Preliminary Analysis

Usually rate-distortion curves are monotonous and they allow comparing properties of different coders for a given image. It is also possible to analyze properties of a given coder for different images depending upon their complexity. Fig. 2 gives an example of PSNR on CR for four coders (SPIHT, JPEG2000 [28], ADCTC and AGU-M for 512x512 pixel fragment of complex structure. As one can see, the coder ADCTC is the best according to the metric PSNR (Fig. 2) but AGU-M is the best according to the metric PSNR-HVS-M (Fig. 3).

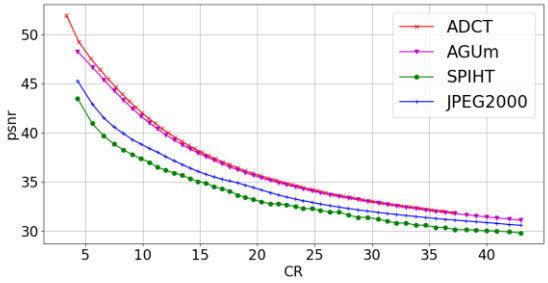

Fig. 2. Dependence of PSNR on CR for four image compression techniques

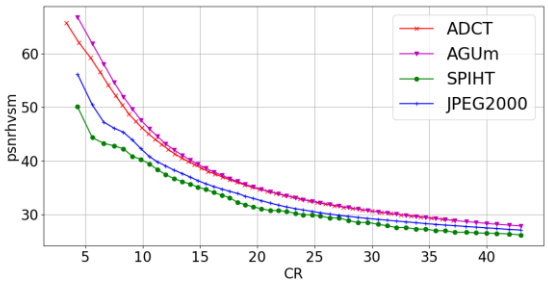

Fig. 3. Dependence of PSNR-HVS-M on CR for four image compression techniques

It is also worth recalling that invisibility thresholds for these metrics are 36 dB and 41 dB, respectively. Then, CR can be about 40 according to PSNR and about 15 according to PSNR-HVS-M. We rely more on PSNR-HVS-M since it is essentially more adequate to visual quality. Certainly, CR also depends upon a coder.

B. Noise Properties

Compression of noisy images has several peculiarities discovered more than twenty years ago [30-32]. It has been shown that lossy compression being applied to noisy images has specific filtering effect that can be considered as positive. Meanwhile, the impact is positive only under certain conditions – if distortions of information content are not large.

There are different approaches to lossy compression in this case. In particular, it is possible to carry out compression in the neighborhood of the so-called optimal operation point if it exists. Meanwhile, for our case, another approach seems reasonable – MSE of introduced distortions should be sufficiently smaller than equivalent variance of the noise. Noise properties have been studied in our paper [28] and it has been demonstrated that noise is spatially correlated and signal dependent. Equivalent variance depends on imaging mode and mean level of entire image or a considered image

fragment. Equivalent variance changes from 10-20 to 100-200 for different considered fragments [28].

It is worth explaining here why we are interested in compression of image fragments. First, large size images are analyzed by doctors using different type of devices including those ones having small screen, Then, they actively use image scrolling. Second, not all parts of large size images can be interesting for diagnostic purposes. Often, particular fragments of interest are studied in natural size. Thus, we have to be sure that for none image fragment of large size image distortions are visible.

III. Experimental Results for Image Fragments

Large size images presented in Fig. 1 have been divided into 20 fragments of size 512x512 pixels and different dependences have been obtained for them. Scaling factor which is a specific QS for the considered coder has been varied from 1 to 29 with the step equal to unity. Then, PSNR, PSMR-HVS-M, MS SSIM and CR have been determined for each fragment and each QS. So, let us present the obtained data and analyze them.

Data for PSNR depending on QS are given in Fig. 4. An obvious tendency to PSNR reduction with QS increasing is observed. For the same QS, PSNR values vary in rather wide limits where the smallest values are observed for the most complex structure fragments and/or if noise intensity is the highest. According to the obtained data, QS should be about 8 to provide invisibility of introduced distortions with high probability.

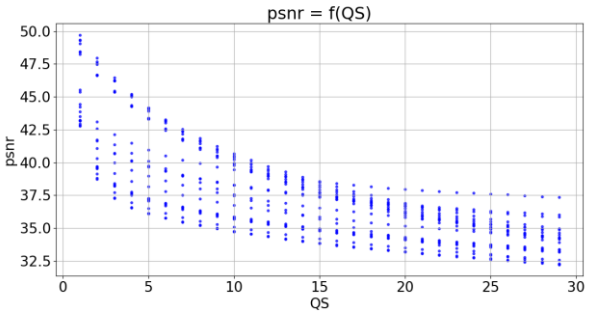

Fig. 4. Data for PSNR on QS for twenty image fragments compressed by AGU-M

Fig. 5 presents similar data for MS SSIM on QS. As one can see, visual quality decreases if QS increases. The conclusion based on MS SSIM data is the same – QS should be about 8 or smaller to guarantee invisibility of distortions.

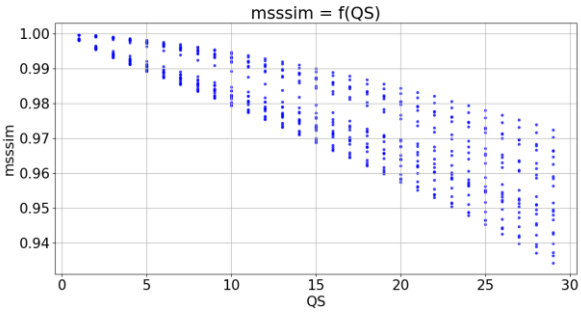

Fig. 5. Data for MS-SSIM on QS for twenty image fragments compressed by AGU-M

It can be also interesting to see what CR are provided by the analyzed coder and what are image quality characteristics in this case. The obtained data are presented in Figures 6-8. Their analysis shows the problems of the approach mentioned in Introduction where researchers recommend to set CR not larger than a recommended one to avoid appearance of visible distortions. According to this approach, it is not reasonable to produce CR>10 – then the considered metrics are practically always above the corresponding distortion invisibility thresholds. Meanwhile, analysis shows that there many cases when the image fragment can be compressed with CR about 20 or even larger providing that image quality is acceptable.

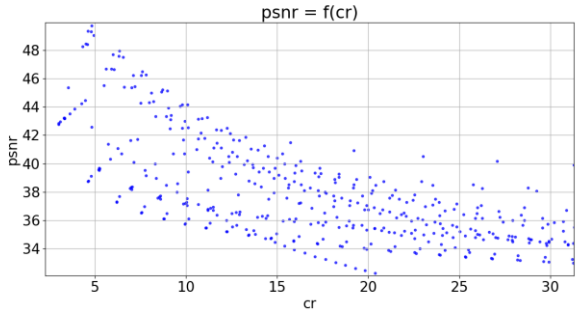

Fig. 6. Data for PSNR on CR for twenty image fragments compressed by AGU-M

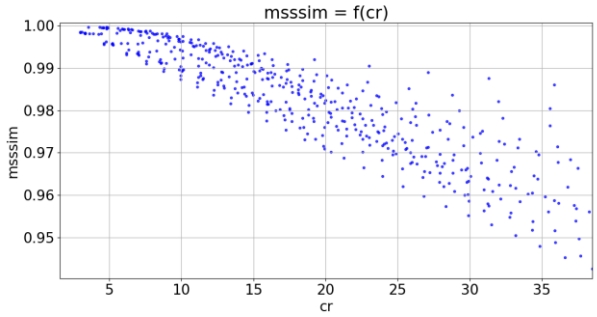

Fig. 7. Data for MS-SSIM on CR for twenty image fragments compressed by AGU-M

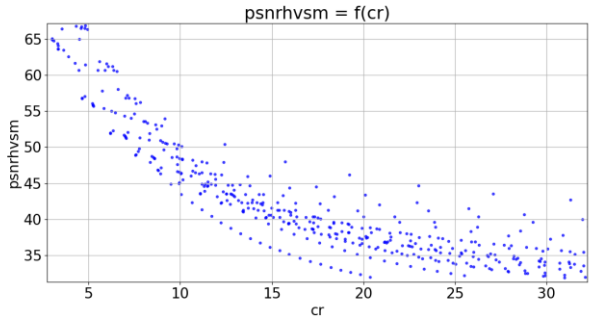

Fig. 8. Data for PSNR-HVS-M on CR for twenty image fragments compressed by AGU-M

Finally, Fig. 9 presents the most important results. These are data for PSNR-HVS-M metric for different QS. These results are in good agreement with data in Figures 4 and 5 and conclusions drawn from them QS should be between 8 and 9. To provide correctness of comparisons, we have found QS that provides the same mean PSNR-HVS-M (equal to 42.5 dB) as in [20]. This QS is equal to 8.8. Its use provides variation of PSNR-HVS-M in the limits from 41.1 to 45.1 (more narrow than in [20]) and CR variation in the

limits from 9.4 to 35.0 (both minimal and maximal values are larger than the corresponding values in [20], 7 and 21, respectively). Thus, three benefits are provided simultaneously compared to the method [20] – more accurate providing of the desired quality, larger CR and, finally, faster compression since AGU-M compresses images by about 4.7 times faster and decompresses by about 1.2 times faster than ADCTC.

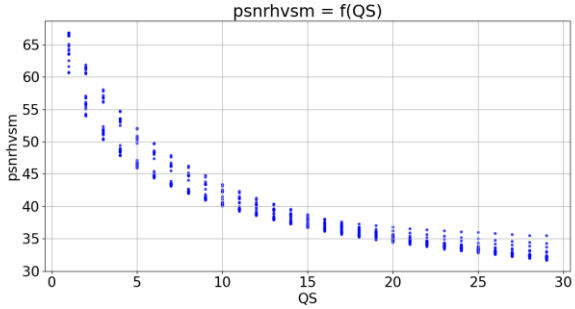

Fig. 9 Data for PSNR-HVS-M on QS for twenty image fragments compressed by AGU-M

IV. Experiments with Experts

Despite reasonable adequateness of the used visual quality metrics, it was necessary to verify the obtained results by attracting specialists that are experts in dental image analysis and diagnostics. Recall that panoramic X-ray is a unique technology that allows a dentist to see both jaws and associated structures. Then, a good quality image is the main tool for correct diagnosis. Also recall that the research methodology consists of four main stages, i.e. clinical examination of a patient, radiographs data collection, image evaluation and result validation. The first step was done at the University Dental Center, Kharkiv National Medical University, Ukraine. All procedures carried out in the dental office have been performed in accordance with the protocols for the provision of dental care to the population in Ukraine. The standard procedure include questioning the patient (if a child, then both parents), clinical examination using standard equipment, and indications for X-ray examination (panoramic X-ray, lateral cephalography, if necessary).

In our case, the total amount of patients undergoing diagnostic X-ray examination was equal to 132. After clinical examination, the patient visited the diagnostic radiographic laboratory, where he/she has underwent the X-ray examination (equipment - The Veraview X800, Morita, Japan) according to the list of indications. The total amount of X-ray images that were evaluated by specialists was equal to 132 (104 orthopantomography images and 28 lateral cephalograms). After the radiographic examination, its results were sent to the University Dental Center by email. Image IDs such as name and gender were not accompanied to protect patient privacy. The images file format was limited to JPG or DICOM, and they were sent by email as an attachment.

To ensure an effective assessment, dentists who have worked in dental clinic for three or more years have evaluated the radiographic images. Prior to this study, seven dentists (orthodontists and pedodontists) were trained to evaluate radiographic images, and objective criteria for image quality were discussed. All dentists (evaluators) have rated the overall quality of the X-ray image into the following categories: 1. optimal for diagnosis, 2. adequate for diagnosis, 3. poor but possible for diagnosis, and 4. unrecognizable, insufficient for diagnosis (the classification was based on the Clinical Image Quality Evaluation Chart).

After clinically examining the patients and obtaining an image, doctors visually evaluated the radiographic image on a computer monitor or smartphone using the maximum zooming of the image. The first stage of the experiment - the dentists analyzed the images anonymously, without information about the type of image - "original" or "compressed" in accordance with the established qualification criteria. The second step was a detailed analysis of known compressed and original images and a qualification assessment.

The results of the first step of the experiment (anonymous evaluation) have showed that 84 images were considered “optimal for diagnosis” according to evaluation criteria. 35 were “adequate for diagnosis” and 13 were “poor but diagnosable”. The most important result for clinicians was that no image was not classified as “unrecognizable”.

During the second step of the experiment, after comparison of "original" or "compressed" images, practically the same result was observed. According to the grades of evaluation, almost all the images were referred to the same groups. One image, after a proper evaluation of the clinicians, moved from “poor but diagnosable” to “adequate for diagnosis”. So even in cases where minor changes were found, they were not associated with a loss in the quality of useful diagnostic information.

Let us present some results. Fig. 10 shows the fragment with simple structure and, mostly, low noise for which the largest CR has been attained.

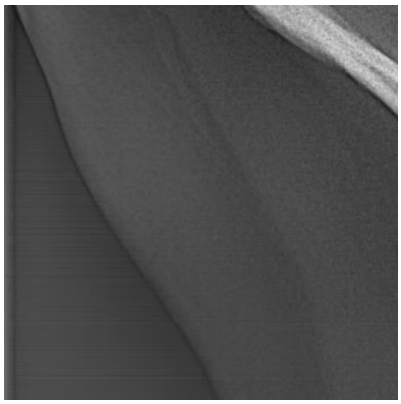

Fig. 10 The image fragment for which the largest CR=34.96 has been attained; PSNR-HVS-M=41.99 dB, SF=8.8 for AGU-M

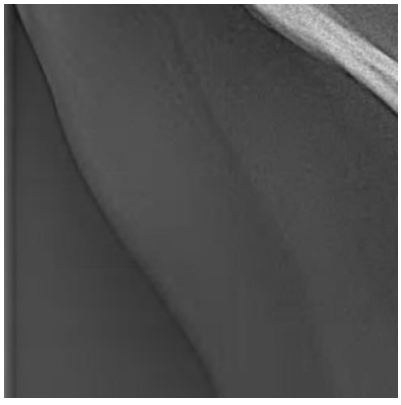

Fig. 11 The image fragment for which SF=20, CR=119, PSNR-HVS-M=36.78 dB

Fig. 12 The image fragment for which the smallest CR=9.38 has been attained; PSNR-HVS-M=45.14 dB, SF=8.8 for AGU-M

Fig. 11 shows what happens if SF is sufficiently smaller than recommended. Comparison of images in Figures 10 and 11 indicates that distortions are visible. Finally, Fig. 12 demonstrates an example of complex structure fragment compressed with small CR.

V. Conclusions

In this paper, we have put forward the approach to visually lossless compression of dental images. It uses the DCT-based coder AGU-M. The advantages of this approach are that it is fast, non-iterative, its CR is adaptive to image complexity, and a desired quality is provided with a rather high accuracy. This guarantees that introduced distortions are invisible and diagnostically important information is preserved.

References

[1] D. A. Madsen, Engineering Drawing & Design, Clifton Park, NY: Delmar. p. 10., 2012, ISBN 978-1111309572.

[2] I. Blanes, E. Magli, J. Serra-Sagrista, “A Tutorial on Image Compression for Optical Space Imaging Systems”, IEEE Geosci. Remote Sens. Mag. 2014, 2, pp. 8–26.

[3] L. Zhang, L. Zhang, X. Mou, and D. Zhang, “FSIM: A feature similarity index for image quality assessment”, IEEE Trans. Image Process., 2011, vol. 20, no. 8, pp. 2378–2386.

[4] E. V. Bataeva, “Flanering and video mania: Modern and postmodern visual practices”, Voprosy Filosofii, 2012, 11, pp. 61–68.

[5] K. Okarma, J. Fastowicz, “Computer Vision Methods for Non-destructive Quality Assessment in Additive Manufacturing”, Progress in Computer Recognition Systems, Springer: CORES 2019. Advances in Intelligent Systems and Computing, 2019; Vol. 977, pp. 11–20

[6] P. M. de Azevedo-Marques, A. Mencattini, M. Salmeri and R. M. Rangayyan, Medical Image Analysis and Informatics: Computer-Aided Diagnosis and Therapy, CRC Press, 2017.

[7] C. Guy and D. Fytche, "An Introduction to the principles of medical imaging. Revised edition", Imperial College Press, 2005, pp. 267-294.

[8] P. Suetens, Fundamentals of Medical Imaging, Cambridge University Press, 2009.

[9] V. Gargin, R. Radutny, G. Titova, D. Bibik, A. Kirichenko and O. Bazhenov, "Application of the computer vision system for evaluation of pathomorphological images," 2020 IEEE 40th International Conference on Electronics and Nanotechnology (ELNANO), Kyiv, Ukraine, 2020, pp. 469-473, doi: 10.1109/ELNANO50318.2020.9088898.

[10] Stuart C. White and Michael J. Pharoah, Oral Radiology: Principles and Interpretation, Elsevier, 2014.

[11] A. Nechyporenko, V. Reshetnik, V. Alekseeva, N. Yurevych, R. Nazaryan and V. Gargin, "Assessment of Measurement Uncertainty of the Uncinated Process and Middle Nasal Concha in Spiral Computed Tomography Data," 2019 IEEE International Scientific-Practical Conference Problems of Infocommunications, Science and Technology (PIC S&T), Kyiv, Ukraine, 2019, pp. 585-588.

[12] S. Jayachandran, “Digital Imaging in Dentistry: A Review”, Contemp. Clin. Dent., 2017, 8, pp. 193–194.

[13] J. Anthony Seibert, “Archiving, Chapter 2: Medical Image Data Characteristics”, Soc. Imaging Inform. Med, 2020, pp. 1-7.

[14] Diagnostic and Imaging Equipment | MORITA Available online: https://www.jmoritaeurope.de/en/products/diagnostic-and-imaging-equipment-overview/ (accessed on Oct 19, 2020).

[15] V. F. Sanchez Silva, Advances in medical image compression : Novel schemes for highly efficient storage, transmission and on demand scalable access for 3D and 4D medical imaging data, PhD Thesis, University of British Columbia, 2010.

[16] A. C. Flint, "Determining optimal medical image compression: Psychometric and image distortion analysis", BMC Med. Imaging, 2012, pp.12–24.

[17] D. A. Koff, H. Shulman, "An overview of digital compression of medical images: Can we use lossy image compression in radiology?", J. Assoc. Can. Radiol., 2006, 57, pp. 211–217.

[18] A. Fidler, B. Likar, "What is wrong with compression ratio in lossy image compression?", Radiology., 2007, pp. 245-299.

[19] F. E. Eraso, M. Analoui, A. B. Watson, R. Rebeschini, "Impact of lossy compression on diagnostic accuracy of radiographs for periapical lesions", Oral Surg. Oral Med. Oral Pathol. Oral Radiol. Endodontol., 2002, 93, pp. 621–625.

[20] S. Krivenko, V. Lukin, O. Krylova, L. Kryvenko, K. Egiazarian, A Fast Method of Visually Lossless Compression of Dental Images, Appl. Sci., 2021, 11(1), 135.

[21] R. Braunschweig, I. Kaden, J. Schwarzer, C. Sprengel, K. Klose, "Image data compression in diagnostic imaging: International literature review and workflow recommendation", ROFO. Fortschr. Geb. Rontgenstr. Nuklearmed., 2009, 181, pp. 629–636.

[22] D. Jayaraman, A. Mittal, A. K. Moorthy, and A. C. Bovik, “Objective quality assessment of multiply distorted images,” in Proc. Asilomar Conf. Signals, Systems and Computers, 2012, pp.1693-1697.

[23] N. Ponomarenko, V. Lukin, J. Astola, K. Egiazarian, "Analysis of HVS-Metrics’ Properties Using Color Image Database TID2013", In Advanced Concepts for Intelligent Vision Systems; Springer: ACIVS 2015. Lecture Notes in Computer Science, 2015; Vol. 9386, pp. 613–624.

[24] Z. Wang, E. P. Simoncelli and A. C. Bovik, "Multiscale structural similarity for image quality assessment", Proc. IEEE Conf. Rec. 37th Asilomar Conf. Signals Syst. Comput., 2003, pp. 1398-1402.

[25] N. Ponomarenko, F. Silvestri, K. Egiazarian, M. Carli, J. Astola and V. Lukin, "On between-coefficient contrast masking of dct basis functions", Proc. 3rd Int. Workshop Video Process. Quality Metrics Consum. Electron., 2007, 4p.

[26] A. Zemliachenko, N. Ponomarenko, V. Lukin, K. Egiazarian and J. Astola, "Still Image/Video Frame Lossy Compression Providing a Desired Visual Quality", Multidimensional Systems and Signal Processing, 2015, 22, pp. 697–718.

[27] N.N. Ponomarenko, V.V. Lukin, K.Egiazarian, J. Astola, "ADCTC: a new high quality DCT based coder for lossy image compression", CD ROM Proceedings of LNLA, Switzerland, August 2008, 6 p.

[28] S. Krivenko, F. Li, V. Lukin, B. Vozel and O. Krylova, "Prediction of Visual Quality Metrics in Lossy Image Compression," 2020 IEEE 40th International Conference on Electronics and Nanotechnology (ELNANO), Kyiv, Ukraine, 2020, pp. 478-483.

[29] Y. Blau and T. Michaeli, "Rethinking Lossy Compression: The Rate-Distortion-Perception Tradeoff", Proceedings of the 36th International Conference on Machine Learning PMLR 97, 2019, pp. 675-685.

[30] O. K. Al-Shaykh and R. M. Mersereau, "Lossy compression of noisy images," in IEEE Transactions on Image Processing, 1998, vol. 7, no. 12, pp. 1641-1652.

[31] J. E. Odegard, H. Guo, C. S. Burrus, R. G. Baraniuk, "Joint Compression and Speckle Reduction of SAR Images using Embedded Zerotree Models", In Workshop on Image and Multidimensional Digital Signal Processing; IDFL:Belize; 1996; pp. 80–81.

[32] S. G. Chang, Bin Yu and M. Vetterli, "Adaptive wavelet thresholding for image denoising and compression," in IEEE Transactions on Image Processing, 2000, vol. 9, no. 9, pp. 1532-1546.